A Temperature-Dependent Kinetics Study of the Important Stratospheric Reaction $O(^3P) + NO_2 \rightarrow O_2 + NO$

E. G. Estupiñán,[†] J. M. Nicovich,[‡] and P. H. Wine*[,†,‡]

School of Earth and Atmospheric Sciences and School of Chemistry and Biochemistry, Georgia Institute of Technology, Atlanta, Georgia 30332

Received: May 21, 2001; In Final Form: August 14, 2001

A laser flash photolysis-resonance fluorescence technique has been employed to investigate the kinetics of the important stratospheric reaction $O(^3P) + NO_2 \rightarrow O_2 + NO$ (k_1) as a function of temperature (221−425 K) with particular attention paid to obtaining the most accurate values possible for $k_1(T)$. The following Arrhenius expression adequately describes the observed temperature dependence: $k_1(T) = (4.21 \pm 0.25) \times 10^{-12} \exp\{(273 \pm 18)/T\}$ cm^3 molecule^{-1} s^{-1}, where the uncertainties represent precision at the 2σ level. The accuracy of the reported values for $k_1(T)$ is estimated to be ±6% over the entire temperature range investigated. At room temperature the rate coefficient measured in this study is in excellent agreement with that reported in a recent paper by Gierczak et al. [*J. Phys. Chem. A* **1999**, *103*, 877] while the activation energy of the rate coefficient is somewhat more negative than that reported by Gierczak et al. Incorporation of the results of the present study into models of stratospheric chemistry would lead to somewhat lower mid-stratospheric ozone levels than would be obtained using results of previous studies.

Introduction

Active nitrogen constituents, primarily NO and NO_2 (together known as NO_x) play important roles both in the troposphere and stratosphere. In the troposphere, NO_x is necessary for the photochemical production of O_3. In addition, NO_x directly and indirectly affects the concentration of the hydroxyl radical, which is the primary tropospheric oxidant responsible for converting many primary emissions to secondary products. In the stratosphere, NO_x-catalyzed destruction cycles in combination with those involving ClO_x, BrO_x, and HO_x radicals strongly influence the concentration and vertical profile of O_3. The catalytic ozone destruction cycle

$$O(^3P) + NO_2 \rightarrow O_2 + NO \quad (1)$$

$$O_3 + NO \rightarrow O_2 + NO_2 \quad (2)$$

$$\text{Net: } O(^3P) + O_3 \rightarrow 2O_2 \quad (3)$$

is the most important NO_x cycle in the stratosphere. Reaction 1 is the rate-determining step in the cycle and it accounts for the majority of odd-oxygen destruction in the 25 to 40 km altitude regime.[1] Hence, it is desirable to know $k_1(T)$ with a very high degree of accuracy, especially at temperatures that are typical of the mid-stratosphere, i.e., 220−260 K.

While several studies of the kinetics of reaction 1 have been reported in the literature,[2−6] the 1997 NASA panel for chemical kinetics and photochemistry data evaluation[7] suggested that the uncertainties in $k_1(T)$ values remained much higher than desired, particularly at temperatures below 240 K. Uncertainties in $k_1(T)$ have been identified as a major source of uncertainty in stratospheric models.[8] The kinetics of reaction 1 were recently reinvestigated by Gierczak et al.[9] These investigators obtained a value for k_1(298 K) that is 10% faster than the previously recommended value, and report that k_1 increases with decreasing temperature more rapidly than suggested by earlier studies. The findings of Gierczak et al.[9] stimulated the present study of the kinetics of reaction 1 with the goal of measuring this critical rate coefficient to a high degree of accuracy over the temperature range 220−425 K.

In this study, kinetic information was obtained by monitoring the temporal profile of oxygen atoms under pseudo-first-order conditions with NO_2 in large excess. Special emphasis was placed on accurate determination of the NO_2 concentration and on measurements of k_1 at stratospheric temperatures.

Experimental Technique

The laser flash photolysis (LFP)-resonance fluorescence (RF) apparatus used in this study was similar to systems previously employed in this laboratory to study atom−molecule reactions involving O atoms.[10] A schematic diagram of the current version of the apparatus is published elsewhere.[11] Important features of the apparatus and experimental approach that are specific to this study are described below.

A Pyrex, jacketed reaction cell with an internal volume of ~150 cm^3 was used in all experiments. The cell was maintained at a constant temperature by circulating ethylene glycol ($T >$ 298 K) or methanol ($T <$ 298 K) from a thermostated bath through the outer jacket. A copper−constantan thermocouple with a stainless steel jacket was periodically injected into the reaction zone through a vacuum seal to measure the gas temperature under the precise pressure and flow rate conditions of the experiment. The thermocouple was retracted during kinetic experiments and the temperature measurement in the reaction zone is estimated to be accurate to ±1 K.

* Author to whom correspondence should be addressed at School of Chemistry and Biochemistry, Georgia Institute of Technology, Atlanta, GA 30332-0400. E-mail: pw7@prism.gatech.edu.
[†] School of Earth and Atmospheric Sciences.
[‡] School of Chemistry and Biochemistry.

10.1021/jp011940o CCC: $20.00
Published on Web 09/27/2001

Oxygen atoms were produced by 355 nm laser flash photolysis of NO_2 using third harmonic radiation from a Nd:YAG laser (Quanta Ray model DCR-2A, pulse width ~6 ns) as the photolytic light source:

$$NO_2 + h\nu \rightarrow O(^3P) + NO \qquad (4)$$

At $\lambda = 355$ nm, the yield of $O(^3P)$ in reaction 4 is known to be unity.[7] An atomic resonance lamp, situated perpendicular to the photolysis laser, excited resonance fluorescence in the photolytically produced atoms. The resonance lamp consisted of an electrodeless microwave discharge through ~1 Torr of a flowing mixture containing a trace of O_2 in helium. The flow of a 0.1% O_2 in He mixture and pure He into the lamp were controlled by separate needle valves, thus allowing the total pressure and O_2 concentration to be adjusted for optimum signal-to-noise. Radiation was coupled out of the lamp through a MgF_2 window and into the reaction cell through a MgF_2 lens. Dry N_2 was used as a purge gas in the volume between the lamp window and the reaction cell lens to exclude room air and thus allow transmission of vacuum-UV radiation.

Fluorescence from excited $O(^3P)$ atoms within the reaction zone was collected by a MgF_2 lens on an axis orthogonal to both the photolysis laser beam and the resonance lamp beam and imaged onto the photocathode of a solar blind photomultiplier. The region between the reaction cell and the photomultiplier was purged with dry N_2 and contained a CaF_2 window to prevent detection of Lyman-α emission from the resonance lamp. The fluorescence signals were processed using photon-counting techniques in conjunction with multichannel scaling. For each $O(^3P)$ decay rate measured, 500−5000 temporal profiles were co-added to obtain a well-defined temporal profile. The multichannel analyzer sweep was triggered approximately 3.2 ms prior to the photolysis laser in order to determine the background light level immediately before the laser flash.

To avoid accumulation of photolysis or reaction products, all experiments were carried out under "slow-flow" conditions. The linear flow rate through the reactor was typically 3 cm s^{-1}, and the laser repetition rate was typically 5 Hz. Since photolysis occurred on an axis perpendicular to the direction of flow, no volume element of the reaction mixture was subjected to more than a few laser shots. The reactant and photolytic precursor, NO_2, was flowed into the reaction cell from a 12-L bulb containing dilute mixtures in nitrogen buffer gas, while N_2 was flowed directly from a high-pressure tank. The NO_2/N_2 bulb was blackened to prevent photolysis by room lights.

To minimize systematic error in the NO_2 concentration measurement, two independent methods were employed. In one method, the flow of the NO_2/N_2 mixture and the flow of pure N_2 were both measured with calibrated mass flow meters. The concentration of NO_2 was calculated using measurements of the mass flow rates of the two components of the flow, the total pressure in the reaction cell (measured with a 1000 Torr full scale capacitance manometer), and the temperature in the reaction cell. The mole fraction of NO_2 in the NO_2/N_2 mixture was checked frequently by UV photometry at 366 nm. The photometric measurements were carried out on a separate high vacuum gas handling system employing a mercury penray lamp and a photomultiplier tube equipped with an interference filter to isolate the three Hg transitions at $\lambda \sim 366$ nm from other lamp emissions. The effective NO_2 absorption cross section was measured using the same lamp and filter to be $(6.05 \pm 0.14) \times 10^{-19}$ cm^2 $molecule^{-1}$.

The concentration of NO_2 was also determined by in situ long-path absorption measurements both upstream and downstream of the reaction cell. Using a partially reflecting optic, the output beam of the argon ion laser operating at 457.9 nm was split into two approximately equal components which were then multipassed using White cell optics[12] through two separate Pyrex absorption cells. The windows on the absorption cells had antireflection coatings (400−500 nm) and the White cell mirrors were coated for high reflectivity (425−485 nm). For these experiments, the upstream cell was 37.3 cm in length with 52 passes of the laser beam and the downstream cell was 35.5 cm in length with 56 passes. The intensity of the laser light exiting the White cells was continuously monitored by separate silicon photodiodes. To reference the signals from these two photodiodes to the initial intensity of the laser, a thin, glass optic was used to pick off a portion of the laser beam before the beam splitter and direct it onto a third photodiode. Each photodiode was equipped with a stack of thin Teflon diffusers to prevent saturation. The detector signals were electronically amplified and processed through an analog-to-digital card in a personal computer. An electromechanical shutter allowed the laser beam to be periodically blocked in order to measure the small background for each detector. On a separate gas handling system, the NO_2 absorption cross section at 457.9 nm and room temperature was measured using the same Ar^+ laser, a 37.4 cm long absorption cell, and manometrically measured samples of NO_2. Again, the light intensity of the laser beam exiting the absorption cell was referenced to the initial intensity using a pick-off mirror and a second photodiode. Absorption measurements were made over a wide range of $[NO_2]$ (0.11 to 0.87 Torr), path length (1 to 5 passes of the laser beam), and total pressure (N_2 was added for some measurements). The pressure gauges used for these determinations were calibrated by the expansion of known masses of various gases into the known volumes of the gas manifold and absorption cell. Results of both methods of determining the NO_2 concentrations in the kinetics experiments are discussed below.

The N_2 used in this study was UHP grade with a minimum purity of 99.999%; it was used as supplied. NO_2 was prepared by reacting NO with excess O_2 and leaving the mixture overnight. NO_2 was then collected in a liquid nitrogen cooled trap while O_2 and other impurities were pumped away. NO and O_2 had minimum stated purities of 99.0% and 99.996%, respectively.

Results and Discussion

1. NO_2 Concentration Results. The NO_2 absorption cross section at the argon ion laser wavelength (457.9 nm) was determined thirty-two times in order to maximize the precision of the measurement. These results are summarized in Figure 1, where the calculated NO_2 cross section is plotted as a function of absorbance. Two parameters were varied to ensure that the measured NO_2 cross section was independent of initial conditions; these were the initial NO_2 pressure and the total laser absorption path length. No systematic change in cross section results was observed. The NO_2 concentration was corrected for the formation of N_2O_4 using the equilibrium constant recommended by the NASA panel.[7] The corrections were very small (<1%). Calibration of the pressure gauge used in the cross section measurements showed that the pressure reading was 1.9 ± 2.5% higher than expected from masses of the expanded ideal gases (uncertainty is 2σ). Therefore, the NO_2 cross section was corrected upward by 1.9%. Two experiments were performed at a total pressure of 100 Torr using N_2 as the buffer gas (open symbols in Figure 1). From our experiments, the NO_2 absorption cross section at 457.9 nm is measured to be $(5.06 \pm 0.08) \times$

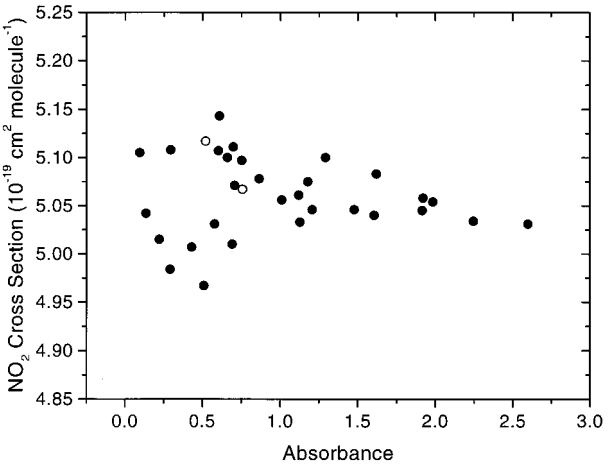

Figure 1. Plot of the calculated NO_2 absorption cross section at the argon ion laser wavelength (457.9 nm) versus absorbance. Solid circles indicate absorption cross-section measurements made with only NO_2, while open circles indicate absorption cross-section measurements made with NO_2/N_2 mixtures at a total pressure of 100 Torr.

TABLE 1: Quantitative Comparison of k_1 Obtained from This Study Using the NO_2 Concentration Determined by Absorption with the NO_2 Concentration Determined by Flow

T[a]	$k_{absorption}$[b]/k_{flow}[c]	T[a]	$k_{absorption}$[b]/k_{flow}[c]
425	1.01	295	0.98
406	1.00	295	1.06
374	1.01	295	1.01
346	0.99	295	1.05
324	1.02	271	1.01
294	0.99	244	1.01
295	1.00	221	1.00
295	1.01		

[a] Units are T (K). [b] Rate coefficient for reaction 1 determined using an average between the upstream and downstream NO_2 concentrations measured by absorption. [c] Rate coefficient for reaction 1 determined using the NO_2 concentration measured by flow.

10^{-19} cm^2 molecule^{-1}, where the stated uncertainty represents precision at the 95% confidence level. It is difficult to make a direct comparison between the NO_2 cross section obtained at 457.9 nm in this study and NO_2 cross sections obtained in previous studies because of the higher resolution of our measurement and the structured nature of the NO_2 absorption spectrum. Nonetheless, there is reasonably good agreement between our measured NO_2 cross section and the 0.5 nm averages reported by Harder et al.,[13] $\sim 5.1 \times 10^{-19}$ cm^2 molecule^{-1}, and Schneider et al.,[14] $\sim 4.5 \times 10^{-19}$ cm^2 molecule^{-1}.

In the kinetics experiments, excellent agreement was found between the NO_2 concentration measurements made by in situ absorption and the corresponding concentrations calculated from flow and pressure measurements. Furthermore, excellent agreement was found between the upstream and downstream NO_2 concentrations determined by absorption. Table 1 shows the ratio of the rate coefficient for reaction 1 determined using an average between the upstream and downstream NO_2 concentrations measured by absorption to the same rate coefficient determined using the NO_2 concentration measured by flow. The difference between the measurements was typically less than 2% and was never greater than 6%. Hence, the three NO_2 measurements were averaged, $([NO_2]_{upstream} + [NO_2]_{downstream} + [NO_2]_{flow})/3$, to yield a single NO_2 concentration determination for each pseudo-first-order decay rate. Since the experiments were performed under flow conditions, the NO_2 concentration measured in each of the two absorption cells was corrected to the pressure in the reaction cell. These pressure drop corrections were small (<2%) and could be made very accurately.

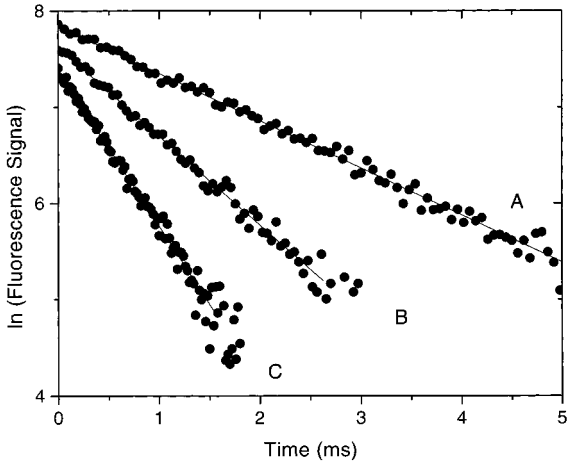

Figure 2. Typical resonance fluorescence temporal profiles observed in the study of reaction 1. Experimental conditions: $T = 244$ K; $P = 15$ Torr; $[NO_2]$ in units of 10^{13} molecules cm^{-3} = (A) 3.09, (B) = 6.58, (C) = 12.20; number of laser shots averaged = (A) 800, (B) = 1000, (C) = 2000. Solid lines are obtained from least squares analyses and give the following first-order decay rates in units of s^{-1}: (A) 490, (B) 940, (C) 1620.

2. Kinetic Results. All the experiments were carried out under pseudo-first-order conditions with NO_2 in large excess over $O(^3P)$. Thus, in the absence of secondary reactions that enhance or deplete the $O(^3P)$ atom concentration, the $O(^3P)$ atom temporal profile is dominated by the reactions

$$O(^3P) + NO_2 \rightarrow O_2 + NO \quad (1)$$

$$O(^3P) \rightarrow \text{loss by diffusion from the detector field of view and/or reaction with background impurities} \quad (5)$$

Integration of the rate equations for the above scheme yields the following simple relationship:

$$\ln\{S_0/S_t\} = (k_1[NO_2] + k_5)t = k't \quad (6)$$

In eq 6, S_0 is the $O(^3P)$ fluorescence signal at a time shortly after the laser fires and S_t is the $O(^3P)$ fluorescence signal at time t. The bimolecular rate coefficient, k_1, is determined from the slope of a k' vs $[NO_2]$ plot.

$O(^3P)$ atom decays were found to be exponential and the pseudo-first-order $O(^3P)$ decay rates were found to increase linearly with increasing NO_2 concentration except at $T < 240$ K (see discussion below). These kinetic observations are consistent with eq 6. Furthermore, observed decay rates were independent of laser photon fluence. This set of observations strongly supports the contention that reactions 1 and 5 are the only processes which affected the post-laser-flash $O(^3P)$ time history in the experiments performed at $T > 240$ K and the dominant processes at $T < 240$ K.

Typical observed oxygen atom temporal profiles are shown in Figure 2 and typical plots of k' versus $[NO_2]$ are shown in Figure 3. The kinetic data for reaction 1 are summarized in Table 2. k_1 was measured at 10 different temperatures, ranging from 221 to 425 K. Some experiments were performed at a very low NO_2 flow through the system (i.e., not measurable by either absorption or flow methods) in order to measure the $O(^3P)$ atom background decay rate in essentially the absence of NO_2. In these experiments a few percent of NO_2 was lost due to

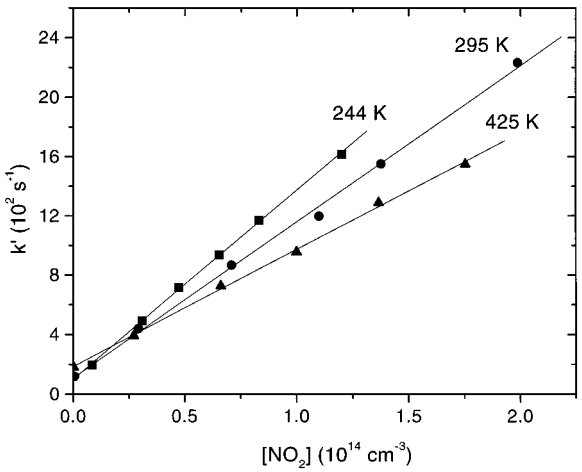

Figure 3. Typical plots of k' versus $[NO_2]$ for data obtained in the study of reaction 1. Solid lines are obtained from least squares analyses; their slopes give the bimolecular rate coefficients in units of 10^{-12} cm^3 molecule^{-1} s^{-1}: 12.7 at 244 K, 10.5 at 295 K, and 7.89 at 425 K.

TABLE 2: Summary of Kinetic Data for the Reaction $O(^3P) + NO_2 \rightarrow O_2 + NO$

T^a	P^a	$[NO_2]^{a,b}$	$[O]_0^{a,c}$	no. of expts.^{d}	range of k'^a	$k_1^{a,e}$
425	15	5−1750	3.0	6	180−1550	7.89 ± 0.29
406	15	44−3010	3.6	7	190−2600	8.17 ± 0.40
374	15	6−1780	3.0	6	140−1700	8.82 ± 0.14
346	15	5−3500	4.0	8	170−3450	9.50 ± 0.32
324	15	0−1780	3.0	6	120−1850	9.68 ± 0.21
294	15	380−3700	3.3	5	530−3980	10.4 ± 0.2
295	15	0−2010	3.2	6	120−2230	10.5 ± 0.5
295	15	0−1760	1.7	6	94−1970	10.6 ± 0.2
295	15	0−2700	8.9	7	94−2970	10.6 ± 0.2
295	15	0−1620	3.1	6	95−1890	10.9 ± 0.3
295	15	0−1700	3.1	6	130−2000	10.9 ± 0.3
295	15	0−1700	3.1	6	120−2050	10.9 ± 0.4
271	16	0−2860	3.2	7	95−3370	11.6 ± 0.3
244	15	0−1200	2.9	7	90−1620	12.8 ± 0.3
221	15	0−700	3.1	6	90−1110	14.3 ± 0.4

[a] Units are T (K), P (Torr); concentrations (10^{11} per cm^3), k' (s^{-1}), k_1 (10^{-12} cm^3 molecule^{-1} s^{-1}). [b] Average concentration based on flow and absorption measurements. A value of zero indicates that the NO_2 concentration was below our detection limit. [c] Average concentration for each reported value of k calculated based on the measured laser fluence and NO_2 concentration. [d] expt ≡ determination of a single pseudo-first-order decay rate. [e] Uncertainties are 2σ and represent precision only.

photolysis because very high laser powers were needed to obtain a measurable fluorescence signal. In all other experiments the NO_2 concentration was always in large excess over the $O(^3P)$ atom concentration (pseudo-first-order conditions). In the room-temperature experiments (294−295 K), the initial $O(^3P)$ concentration was varied by about a factor of 5 [$(1.7-8.9) \times 10^{11}$ atoms cm^{-3}] resulting in no observed systematic change in the rate coefficients. All the experiments were performed at a relatively low pressure of 15 Torr in order to avoid significant contribution to observed kinetics from the addition reaction

$$O(^3P) + NO_2 + M \rightarrow NO_3 + M \qquad (7)$$

The maximum contribution of reaction 7 (at the lowest temperature investigated) is less than 1% based on the 1997 NASA panel[7] recommendation and less than 2% using the value derived from the recent study by Burkholder and Ravishankara.[15]

An Arrhenius plot for reaction 1 is shown in Figure 4. Like many radical−radical reactions, the temperature dependence of

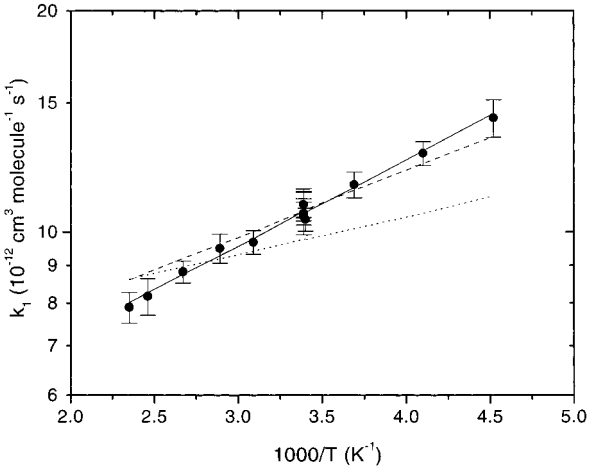

Figure 4. Arrhenius plot for reaction 1 and comparison with the results of Gierczak et al.[9] and the 1997 NASA panel[7] recommendation. Solid data points are from this study and error bars represent our best estimate of accuracy. The solid line is obtained from a weighted least-squares analysis (of data from this study only) and represents the Arrhenius expression given in the text. The dashed line represents the Arrhenius expression reported by Gierczak et al.[9] and the dotted line represents the Arrhenius expression recommended by the NASA panel[7] in 1997.

the rate coefficient for reaction 1 is characterized by a small negative activation energy. A linear least-squares analysis of the ln k_1 vs $1/T$ data gives the following Arrhenius expression:

$$k_1(T) = (4.21 \pm 0.25) \times 10^{-12} \exp\{(273 \pm 18)/T\} \text{ cm}^3 \text{ molecule}^{-1} \text{ s}^{-1} \qquad (8)$$

Uncertainties in the above expression are 2σ and represent precision only. These uncertainties refer to the Arrhenius parameters only. Error estimates for individual rate coefficients are derived below.

The temperature dependence of k_1 can also be parametrized as $k_1(T) = A(T/300)^{-n}$ where T is in units of degrees Kelvin:

$$k_1(T) = (10.57 \pm 0.12) \times 10^{-12} (T/300)^{-(0.85 \pm 0.06)} \text{ cm}^3 \text{ molecule}^{-1} \text{ s}^{-1} \qquad (9)$$

Again, uncertainties in the above expression are 2σ and represent precision only.

At temperatures below 240 K, it becomes necessary to consider the effect of NO_2 dimerization on observed kinetics.

$$NO_2 + NO_2 \leftrightarrow N_2O_4 \qquad (10)$$

Unfortunately, the uncertainty in the equilibrium constant, K_{10}, is very large at low temperatures,[7] thus making quantitative evaluation of the concentration of NO_2 and N_2O_4 in the reaction cell difficult. To shed some light on this problem, we carried out a set of experiments at $T = 210$ K where $O(^3P)$ kinetics were studied over a wide range of concentrations of NO_2 monomer units. As expected, and as shown by the solid symbols in Figure 5, the slope of a plot of k' vs [NO_2 monomer units] decreased with increasing [NO_2 monomer units]. The rate coefficient for the reaction

$$O(^3P) + N_2O_4 \rightarrow \text{products} \qquad (11)$$

is thought to be much smaller than k_1, i.e., $k_{11} < 2 \times 10^{-12}$ cm^3 molecule^{-1} s^{-1} at 199 K.[6] Assuming this to be the case,

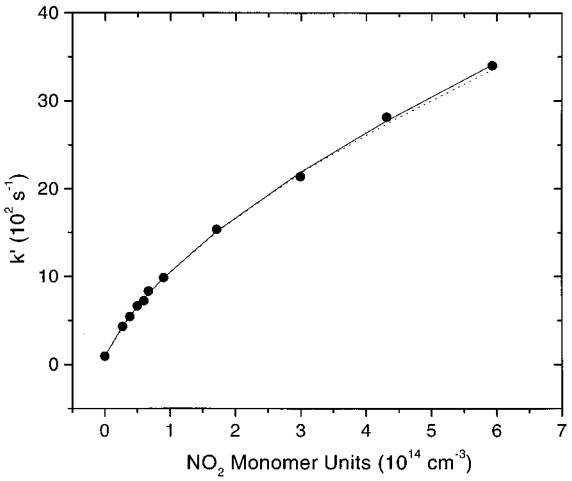

Figure 5. Plot of k' versus [NO_2 monomer units] for data obtained in the study of the NO_2 dimerization equilibrium constant, K_{10}, at $T =$ 210 K. The solid curve is obtained from a nonlinear fit analysis. k_{11} was fixed to 2.0×10^{-12} cm^3 molecule^{-1} s^{-1}. Results of the fit are the following: $k_1 = 1.57 \times 10^{-11}$ cm^3 molecule^{-1} s^{-1}, and $K_{10} = 6.77 \times 10^{-15}$ cm^3 molecule^{-1}. The dotted curve is obtained from a nonlinear fit analysis by fixing k_{11} to zero. Results of this fit are the following: $k_1 = 1.40 \times 10^{-11}$ cm^3 molecule^{-1} s^{-1}, and $K_{10} = 3.23 \times 10^{-15}$ cm^3 molecule^{-1}.

our data were fit to an equation of the form

$$k' = k_1[NO_2] + k_{11}[N_2O_4] + k'_0 \quad (12)$$

where k'_0 was measured to be 94 s^{-1} using a very small concentration of NO_2 ($<1 \times 10^{12}$ molecules cm^{-3}) and [NO_2] is expressed in terms of the dimerization equilibrium constant for reaction 10 and the concentration of NO_2 monomer units. k_1 and K_{10} were allowed to vary and k_{11} was set to 2.0×10^{-12} cm^3 molecule^{-1} s^{-1}. This nonlinear fit to the data is shown as the solid curve in Figure 5. The value for the dimerization equilibrium constant obtained from this fit was 6.77×10^{-15} cm^3 molecule^{-1} and the k_1 value was 1.57×10^{-11} cm^3 molecule^{-1} s^{-1}, which is in excellent agreement with the value for k_1 obtained from extrapolating expression 8 to a temperature of 210 K. The k' vs [NO_2 monomer units] data were also fit assuming k_{11} to be zero (dotted curve in Figure 5). The results of this fit were 3.23×10^{-15} cm^3 molecule^{-1} for K_{10} and 1.40×10^{-11} cm^3 molecule^{-1} s^{-1} for k_1(210 K). This value of K_{10} (i.e., assuming k_{11} to be zero) is in better agreement (only 13% larger) with the currently recommended value for K_{10}(210 K)[7] (see below). In addition, the k' vs [NO_2 monomer units] data at 210 K were also fit allowing all three parameters, k_1, K_{10}, and k_{11}, to vary and we obtained 1.54×10^{-11} cm^3 molecule^{-1} s^{-1} for k_1, 6.04×10^{-15} cm^3 molecule^{-1} for K_{10}, and 1.8×10^{-12} cm^3 molecule^{-1} s^{-1} for k_{11}.

The NASA panel for chemical kinetics and photochemical data evaluation[7] currently recommends the following expression for the temperature dependence of K_{10}:

$$K_{10}(T) = 2.5 \times 10^{-19} \exp(6643/T) \text{ cm}^3 \text{ molecule}^{-1} \quad (13)$$

Assuming that the 298 K equilibrium constant recommended by the NASA panel,[7] is correct and that the 210 K equilibrium constant derived from fitting our kinetic data assuming k_{11} to be 2.0×10^{-12} cm^3 molecule^{-1} s^{-1} is also correct, we obtain the following expression for the temperature dependence of the equilibrium constant:

$$K_{10}(T) = 6.62 \times 10^{-30} \exp(7258/T) \text{ cm}^3 \text{ molecule}^{-1} \quad (14)$$

At $T = 220$ K, the above expression gives an equilibrium constant that is about a factor of 2 larger than the current NASA panel[7] evaluation (expression 13), although well within the evaluated uncertainty of almost a factor of 3. Interestingly, Wollenhaupt and Crowley,[16] in a recent study of the $CH_3O + NO_2$ reaction, arrived at the same conclusion, i.e., the low-temperature value for K_{10} is somewhat larger than currently recommended. In fact, their derived value for K_{10} at 233 K is within 2% of the 233 K value obtained from expression 14. Correcting our NO_2 concentration data for the formation of N_2O_4 at 221 K using expression 14 to obtain K_{10} gives a value for k_1 of 1.47×10^{-11} cm^3 molecule^{-1} s^{-1}. Negligible corrections are needed for the NO_2 concentration at the higher temperatures investigated (i.e., 244 K and above).

Once again, assuming that the 298 K equilibrium constant recommended by the NASA panel[7] is correct and that the 210 K equilibrium constant derived from fitting our kinetic data, assuming k_{11} to be zero, is also correct, we obtain the following expression for the temperature dependence of the equilibrium constant:

$$K_{10}(T) = 3.82 \times 10^{-29} \exp(6735/T) \text{ cm}^3 \text{ molecule}^{-1} \quad (15)$$

At $T = 220$ K, expression 15 gives an equilibrium constant that is only about 12% faster than the current NASA panel[7] evaluation (expression 13). Using expression 15 to correct our NO_2 concentration at 221 K gives a lower limit value for k_1 of 1.37×10^{-11} cm^3 molecule^{-1} s^{-1}.

On the basis of the analysis described above, we report our 221 K rate coefficient as $(1.43 \pm 0.07) \times 10^{-11}$ cm^3 molecule^{-1} s^{-1}, where the stated error includes precision and the uncertainty in the correction for NO_2 dimerization. This value weights the rate coefficient obtained using K_{10} from expression 14 by 60% and the rate coefficient obtained using expression K_{10} from expression 15 by 40%. The higher weight for expression 14 comes from the slightly better fit of k' vs [NO_2 monomer units] at 210 K using a value for k_{11} of 2.0×10^{-12} cm^3 molecule^{-1} s^{-1}.

3. Estimated Accuracy of Reported Rate Coefficients. The two major contributors to the overall accuracy of the rate coefficients in this temperature-dependent study of the $O + NO_2$ reaction are the precision of the rate coefficients and the accuracy of the NO_2 concentration determinations. Examination of Table 2 shows that the precision of the rate coefficients is quite good (typically $\pm 3\%$).

As discussed above, to determine the NO_2 concentration by either "absorption" or "flow," the NO_2 absorption cross section at the chosen wavelength needs to be determined; this is a potential source of error. In the case of the NO_2 absorption measurements, the NO_2 cross section at the argon ion laser wavelength (457.9 nm) was determined with a precision of $\pm 2\%$ at the 95% confidence level. We conservatively estimate that the absolute calibration of the pressure gauge is within $\pm 2.5\%$. There is also some error associated with correcting the NO_2 concentration for the formation of N_2O_4. However, the uncertainty in the equilibrium constant is a negligible source of error in the NO_2 absorption cross section determinations since the contribution of N_2O_4 to the total pressure was less than 1%. The precision of the determinations of both I and I_0 in both the NO_2 cross section measurements at 457.9 and in the determination of the NO_2 concentration during the kinetic experiments

was also quite good, i.e., each one about ±0.5%. As a result, the estimated accuracy of the NO_2 concentration determined by absorption is about ±3.2%. This assessment combines the following factors: an error in the 457.9 nm NO_2 cross section (about ±3.1%), a possible small error in the measurement of the total path length of the argon ion laser beam through the absorption cells of about ±0.4%, and a precision error in the determinations of both I and I_0 during the kinetic experiments (±0.5%).

The error in the NO_2 concentration determined by "flow" is estimated to be about ±4%. This assessment includes a ±3.5% error in the calculation of the NO_2 bulb fraction (which itself includes a ±2% error in the precision of the effective NO_2 cross section for the three Hg atomic lines at $\lambda \sim 366$ nm and a ±2.5% error in the pressure gauge used in the cross section measurements), a ±0.5% error in each one of the two flowmeters, and a ±2% error in the pressure gauge used in the kinetic experiments. Despite our best efforts in deriving a more accurate equilibrium constant for reaction 1 at low temperatures, there is still considerable uncertainty in its determination. Hence, at 221 K, there is an additional ±4% error associated with the choice of K_{10} used to correct the NO_2 concentration for the presence of N_2O_4 in the reaction cell. When all the above errors are propagated, the overall accuracy of each individual rate coefficient is approximately ±6%, and changes very little over the temperature range of our study (221−425 K).

4. Comparison of Reported Rate Coefficients with Literature Values. Figure 4 compares the results of our study of reaction 1 with those of Gierczak et al.[9] and with the 1997 NASA panel[7] recommendation. The k_1(298 K) value of this study agrees within 1% with the result of Gierczak et al.,[9] while the low-temperature rate coefficients are somewhat faster than those reported by Gierczak et al.[9] For example, at $T = 220$ K the rate coefficient obtained from our Arrhenius expression is 7.4% faster than the one reported by Gierczak et al.[9] Nonetheless, the results of this study and of Gierczak et al.[9] are in agreement that the rate coefficient for the $O + NO_2$ reaction is faster at stratospheric temperatures than previously thought.[7] For a critical evaluation of previous $O + NO_2$ rate coefficient measurements, readers are referred to Gierczak et al.[9] and Sander et al.[17]

The study by Gierczak et al.[9] also used the technique of LFP-RF to study the kinetics of reaction 1. In their study, oxygen atoms were produced by 308 nm laser flash photolysis of NO_2 using a XeCl excimer laser. As in this study, kinetic information was obtained by monitoring the temporal profile of oxygen atoms under pseudo-first-order conditions with NO_2 in large excess. To minimize systematic error in the NO_2 concentration measurement, three independent methods were employed: flow rate measurements, absorption, and chemical titration ($NO + O_3 \rightarrow NO_2 + O_2$). In the absorption method, the NO_2 concentration was measured directly in the reactor using UV−visible photometry at 413.4 nm (a D_2 lamp was the light source). This can be compared with our approach where the NO_2 concentration was measured upstream and downstream of the reaction cell using the output of an argon ion laser at 457.9 nm. As discussed above, excellent agreement was found between our upstream and the downstream NO_2 concentration measured by absorption. Our approach to obtaining NO_2 concentrations seems to result in better precision than was obtained by Gierczak et al.[9] although, of course, their measurement of NO_2 in situ in the reaction cell is commendable as an approach for minimizing systematic errors.

Inspection of Figure 4 shows that the temperature dependence of k_1 reported in this study is somewhat more pronounced than the temperature dependence of k_1 reported by Gierczak et al.[9] One possible explanation for this difference concerns the fact that Gierczak et al.[9] measured the NO_2 concentration at the temperature of the kinetic experiment and used measured temperature-dependent absorption cross sections (measured during the course of their study) to convert measured absorbances to NO_2 concentrations. On the other hand, all absorption measurements in this study were at room temperature, and the ideal gas equation of state was employed to convert measured NO_2 concentrations to the reaction cell temperature. Also, the only difference between our value for k_1(221 K) and the one reported by Gierczak et al.[9] appears to be the approach employed to correct for NO_2 dimerization, i.e., they used the recommended[7] low-temperature equilibrium constant whereas we used the approach described above.

5. Implications for Atmospheric Chemistry. Incorporation of the results of this study in models of stratospheric chemistry would lead to somewhat lower ozone levels than would be obtained using the expression for $k_1(T)$ currently recommended by the NASA panel.[17] This is true even though the current recommendation heavily weights the results of Gierczak et al.[9] The biggest impact of our reported rate coefficients is expected in the 23−40 km altitude regime, where temperatures are relatively low and the $O + NO_2$ catalytic cycle dominates odd-oxygen destruction[1]. Some of the consequences of increasing the value of k_1 at stratospheric temperatures, together with updated rate coefficients for the reactions $OH + HNO_3$ (k_{16}) and $OH + NO_2 + M$ (k_{17}), are discussed in a recent modeling study by Portmann et al.[18] These investigators have found that an increase in k_1, combined with the updates in k_{16} and k_{17}, leads to lowering, by about one kilometer, the altitude at which NO_x-catalyzed O_3 removal dominates. In addition, a faster value for k_1 at stratospheric temperatures leads to a decrease of a few percent in total column O_3. The biggest impact is at higher latitudes during the summer months, while no change in the O_3 column is found in the tropics.[18]

Acknowledgment. This research was supported by the National Aeronautics and Space Administration-Upper Atmosphere Research Program through Grant NAG5-8931.

References and Notes

(1) McElroy, M. B.; Salawitch, R. J.; Minschwaner, K. *Planet. Space Sci.* **1992**, *40*, 373.

(2) Davis, D. D.; Herron, J. T.; Huie, R. E. *J. Phys. Chem.* **1973**, *58*, 530.

(3) Slanger, T. G.; Wood, B. J.; Black, G. *Int. J. Chem. Kinet.* **1973**, *5*, 615.

(4) Bemand, P. P.; Clyne, M. A. A.; Watson, R. T. *J. Chem. Soc., Faraday Trans. 2* **1974**, *70*, 564.

(5) Ongstad, A. P.; Birks, J. W. *J. Chem. Phys.* **1984**, *81*, 3922.

(6) Geers-Muller, R.; Stuhl, F. *Chem. Phys. Lett.* **1987**, *135*, 263.

(7) DeMore, W. B.; Sander, S. P.; Golden, D. M.; Hampson, R. F.; Kurylo, M. J.; Howard, C. J.; Ravishankara, A. R.; Kolb, C. E.; Molina, M. J. *Chemical Kinetics and Photochemical Data for Use in Stratospheric Modeling*. Evaluation No. 12; Jet Propulsion Laboratory: Pasadena, CA, 1997.

(8) Dubey, M. K.; Smith, G. P.; Hartley, W. S.; Kinnison, D. E.; Connell, P. S. *Geophys. Res. Lett.* **1997**, *24*, 2737.

(9) Gierczak, T.; Burkholder, J. B.; Ravishankara, A. R. *J. Phys. Chem. A* **1999**, *103*, 877.

(10) Thorn, R. P.; Nicovich, J. M.; Cronkhite, J. M.; Wang, S.; Wine, P. H. *Int. J. Chem. Kinet.* **1995**, *27*, 369, and references therein.

(11) Finlayson-Pitts, B. J.; Pitts, J. N., Jr. *Chemistry of the Upper and Lower Atmosphere*; Academic Press: New York, 2000; p 146.

(12) White, J. U. *J. Opt. Soc. Amer.* **1942**, *32*, 285.

(13) Harder, J. W.; Brault, J. W.; Johnston, P. V.; Mount, G. H. *J. Geophys. Res*. **1997**, *102*, 3861.
(14) Schneider, W.; Moortgat, G. K.; Tyndall, G. S.; Burrows, J. P. *J. Photochem. Photobiol. A* **1987**, *40*, 195.
(15) Burkholder, J. B.; Ravishankara, A. R. *J. Phys. Chem. A* **2000**, *104*, 6752.
(16) Wollenhaupt, M.; Crowley, J. N. *J. Phys. Chem. A* **2000**, *104*, 6429.
(17) Sander, S. P.; Friedl, R. R.; DeMore, W. B.; Golden, D. M.; Kurylo, M. J.; Hampson, R. F.; Huie, R. E.; Moortgat, G. K.; Ravishankara, A. R.; Kolb, C. E.; Molina, M. J. *Chemical Kinetics and Photochemical Data for Use in Stratospheric Modeling*. Evaluation No. 13; Jet Propulsion Laboratory: Pasadena, CA, 2000.
(18) Portmann, R. W.; Brown, S. S.; Gierczak, T.; Talukdar, R. K.; Burkholder, J. B.; Ravishankara, A. R. *Geophys. Res. Lett*. **1999**, *26*, 2387.